Front. Environ. Sci. Eng. 2013, 7(6): 815–826
DOI 10.1007/s11783-013-0503-6

RESEARCH ARTICLE

Size-resolved aerosol ionic composition and secondary formation at Mount Heng in South Central China

Xinfeng WANG[1], Wenxing WANG (✉)[1], Likun XUE[2], Xiaomei GAO[1], Wei NIE[1], Yangchun YU[1], Yang ZHOU[1], Lingxiao YANG[1], Qingzhu ZHANG[1], Tao WANG[2]

1 Environment Research Institute, Shandong University, Jinan 250100, China
2 Department of Civil and Environmental Engineering, Hong Kong Polytechnic University, Hong Kong, China

Abstract To understand the size-resolved aerosol ionic composition and the factors influencing secondary aerosol formation in the upper boundary layer in South Central China, size-segregated aerosol samples were collected using a micro-orifice uniform deposit impactor (MOUDI) in spring 2009 at the summit of Mount Heng (1269 m asl), followed by subsequent laboratory analyses of 13 inorganic and organic water-soluble ions. During non-dust-storm periods, the average $PM_{1.8}$ concentration was 41.8 $\mu g \cdot m^{-3}$, contributing to 55% of the PM_{10}. Sulfates, nitrates, and ammonium, the dominant ions in the fine particles, amounted to 46.8% of the $PM_{1.8}$. Compared with Mount Tai in the North China Plain, the concentrations of both fine and coarse particles and the ions contained therein were substantially lower. When the air masses from Southeast Asia prevailed, intensive biomass burning there led to elevated concentrations of sulfates, nitrates, ammonium, potassium, and chloride in the fine particles at Mount Heng. The air masses originating from the north Gobi brought heavy dust storms that resulted in the remarkable production of sulfates, ammonium, methane sulfonic acid, and oxalates in the coarse particles. Generally, the sulfates were primarily produced in the form of $(NH_4)_2SO_4$ in the droplet mode via heterogeneous aqueous reactions. Only approximately one-third of the nitrates were distributed in the fine mode, and high humidity facilitated the secondary formation of fine nitrates. The heterogeneous formation of coarse nitrates and ammonium on dry alkaline dust surfaces was found to be less efficient than that on the coarse particles during non-dust-storm periods.

Keywords aerosol water-soluble ions, size distributions, secondary formation, dust storm, Mount Heng

Received December 29, 2012; accepted February 27, 2013

E-mail: wenxwang@hotmail.com

1 Introduction

Water-soluble ions are among the major components of atmospheric aerosols [1]. The content and size distributions of inorganic ions and organic acids are crucial for the aerosol characteristics including optical properties, hygroscopicity, acidity, and reactivity, which have potential impacts on the atmospheric visibility, cloud formation, acid precipitation, and human health [2–5]. The chemical composition and abundances of aerosol ions differ from location to location. In polluted urban areas, the secondary sulfates, nitrates, and ammonium are the dominant ions and comprise approximately half of the fine aerosol [6]. In marine areas, chlorides and sodium from sea salts are the most abundant ions in the total suspended particles [7]. In the desert or Gobi region, the dust aerosol primarily comprises crustal substances [8]. The characteristics of the size distribution of aerosol ions, to a certain extent, reflect their sources and the involved atmospheric processes [9]. Typically, the secondary inorganic ions of sulfate and ammonium are primarily produced in the fine particles. However, sodium, chlorides, calcium, and magnesium, which come from the primary emissions of sea salts and ground dust, mostly appear in the coarse particles [10–13]. The size distributions of aerosol ions may alter if the ambient air is influenced by intensive pollutant emissions from anthropogenic or natural sources. For example, massive coal combustion or biomass burning will produce a high concentration peak of chloride in the fine mode [14], and a dust storm may cause high levels of sulfates in the coarse mode [15].

In the past decades, rapid industrialization and urbanization have caused severe particulate pollution in mainland China [16]. The complexity of the size-resolved aerosol ionic composition in the ambient air has raised the demand to conduct relevant field measurements in different areas. So far, the field studies on the size distribution of aerosol

water-soluble ions were mostly made at surface sites, such as the North China Plain [12,14,17–19] and the Pearl River Delta (PRD) [10,20], and only limited studies were performed at high-altitude mountains [13,21]. Mount Heng, a high-elevation mountain (1269 m asl) located in South Central China, is an ideal location to investigate the aerosol concentrations and ionic composition within different size ranges in the upper boundary layer in that region. The air flow at Mount Heng is strongly influenced by the Asian Monsoon [22,23] and shows large variability, particularly during the monsoon transition period in the spring [24]. Because the summit of Mount Heng is far from the concentrated anthropogenic emission regions, the concentrations and size distributions of aerosol ions are possibly strongly affected by the long-range transport of particulate matter and the atmospheric chemical processes during the transport. This situation provides an opportunity to study the influences of air-mass transport on the aerosol ionic compositions at Mount Heng and the involved formation mechanisms.

As part of China's National Basic Research Program on acid rain pollution and control, size-segregated aerosol samples were collected at Mount Heng in spring 2009, and the inorganic ions and organic acids in the aerosols were determined in the laboratory. In this paper, the size-resolved aerosol mass concentrations in spring at Mount Heng were presented, and the size-resolved aerosol ionic compositions were compared with those observed at Mount Tai. The characteristics of the size distribution of aerosol as well as nine inorganic ions and four organic acids were then analyzed in detail for five clustered air masses. The secondary formation of sulfates and nitrates were also investigated for the non-dust-storm periods and the dust-storm events.

2 Experiment and methods

2.1 Measurement site and the air mass trajectories

The field campaign was conducted in spring in the Nanyue Meteorological Station at the summit of Mount Heng (27°18′ N, 112°42′ E). Mount Heng is located in Hunan Province in South China (as marked in Fig. 1), a region that suffers from severe acidic rain [26]. A large industrial zone (i.e., the Changsha-Zhuzhou-Xiangtan city cluster) is situated 70 km to the north of Mount Heng. The PRD and Yangtze River Delta (YRD), two well-known highly

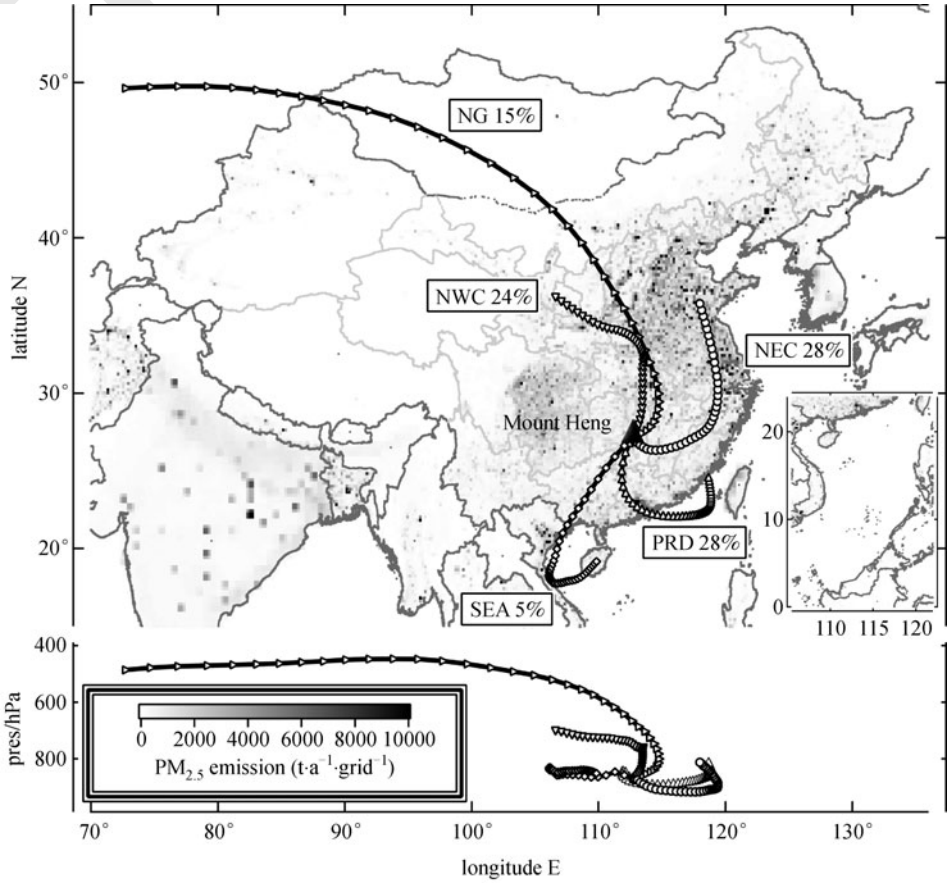

Fig. 1 Map showing the location of the measurement site, the mean five-day backward trajectory clusters, and the Asian emission inventory of $PM_{2.5}$ in 2006 [25]

developed regions in China, are approximately 400 km to the south and 900 km to the north-east, respectively. Mount Heng features high humidity and abundant rainfall in the spring. The detailed information on the meteorological conditions at this site is given in Sun et al. [27].

The analysis of the air mass back trajectory is helpful for understanding the sources and the transport of air pollutants. The hourly five-day back trajectories for the study period were calculated using the Hybrid Single Particle Lagrangian Integrated Trajectory (HYSPLIT, version 4.9) model with Global Data Assimilation System (GDAS) data [28] and were then assorted into different groups according to the transport direction and distance in both horizontal and vertical scales [29]. As shown in Fig. 1, five air mass categories have been identified: fast continental air masses at high altitudes coming from the north Gobi areas (NG, 15%), continental air masses at middle altitudes from the north-western China (NWC, 24%), air masses at low altitudes from northern and eastern China (NEC, 28%), air masses at low altitudes from the PRD region (PRD, 28%), and air masses from Southeast Asia (SEA, 5%). Note that the PRD air masses passed above the sea, and thus the corresponding aerosol samples likely contained abundant sea salts.

2.2 Field measurements and laboratory analyses

In this study, a micro-orifice uniform deposit impactor (MOUDI) (Model 100 with rotator, MSP Corporation, USA) was deployed to collect the aerosol samples in different size ranges at a flow rate of 30 $L \cdot min^{-1}$. There were 8 stages of the MOUDI sampler: >18 μm (inlet), 10–18 μm, 5.6–10 μm, 3.2–5.6 μm, 1.8–3.2 μm, 1.0–1.8 μm, 0.56–1 μm, 0.32–0.56 μm, and 0.18–0.32 μm. A total of 26 sets of size-segregated aerosol samples were collected from March 18 to May 31. The aerosol samples were mostly collected over 24-h periods from 0800 Local Standard Time (LST) in the morning to the next 0800 LST. During the two heaviest dust-storm days, aerosol samples were collected over 12-h periods – from 0800 to 2000 LST for the daytime samples and from 2000 to the next 0800 LST for the nighttime samples. Due to the lack of a water removal device, samples were not collected by the MOUDI sampler during rainy and heavy fog days. Aluminum substrates (ordered from MSP Corporation, USA) were used to collect the aerosol samples in this study. Once the sampling was finished, the substrates were placed in plastic Petri dishes and stored in a refrigerator at a temperature below −5°C for subsequent gravimetric and chemical analyses.

The aluminum substrates were weighed in a weighing room using a microbalance (ME5, Sartorius Corporaton, Germany) before and after collecting the samples. In the laboratory, the size-segregated aerosol samples collected on the substrates were dissolved in deionized water by ultrasonication. Inorganic water-soluble ions in the sample

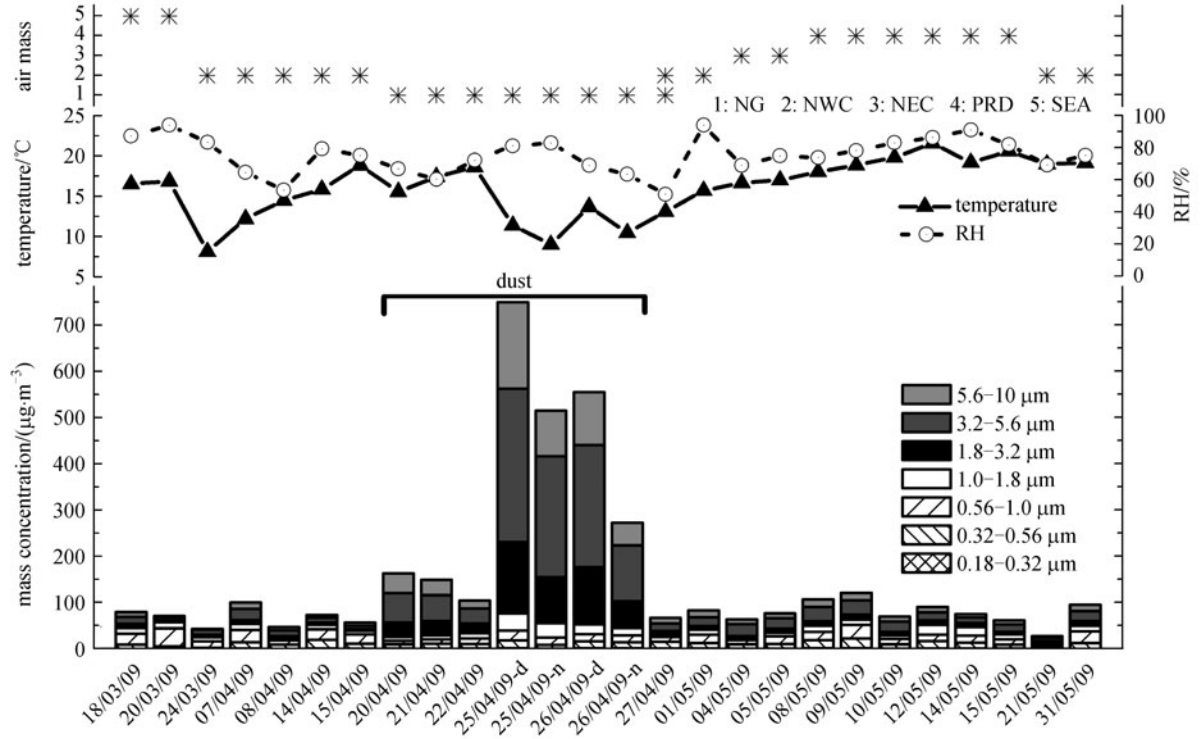

Fig. 2 Time series of size-resolved aerosol mass concentrations in PM_{10} and the corresponding temperature, relative humidity and air mass category in spring at Mount Heng

solutions were detected with an ion chromatograph (ICS 90, Dionex Corporaton, USA). The anions of F^-, Cl^-, NO_3^-, and SO_4^{2-} were analyzed using an AS14A Column and an ASRS 300 Suppresser with an eluent of 3.5 mmol $\cdot L^{-1}$ Na_2CO_3-1.0 mmol$\cdot L^{-1}$ $NaHCO_3$. The cations of Na^+, NH_4^+, K^+, Mg^{2+}, and Ca^{2+} were analyzed using a CS12A Column and a CSRS Ultra II Suppresser with an eluent of 20 mmol$\cdot L^{-1}$ methane sulfonic acid (MSA). Organic water-soluble ions including CHO_2^-, $C_2H_3O_2^-$, $CH_3SO_3^-$, and $C_2O_4^{2-}$ were detected with another ion chromatograph (ICS 2500, Dionex Corporaton, USA), using an AS11-HC Column and an ASRS 300 Suppresser with an eluent of a NaOH solution drawn by a gradient pump. The columns and suppressers used in this study were all ordered from Dionex Corporaton, USA. Note that the organic ions were only determined for some of the aerosol samples. During the chemical analyses using the ion chromatographs, multi-point calibrations were performed for all of these ions every day after the eluent solutions were changed.

Additionally, a number of gas pollutants and meteorological parameters were measured in this study. SO_2 was measured using a pulsed UV fluorescence analyzer (Model 43C, Thermo Electron Corporation, USA), and O_3 using a UV photometric analyzer (Model 49i, Thermo Electron Corporation, USA). Nitric oxide (NO) and NO_2 were measured with a commercial chemiluminescence analyzer (Model 42i, Thermo Electron Corporation, USA) equipped with a photolytic NO_2 converter (blue light converter, Meteorologie Consult Gmbh, Germany). The data on the ambient temperature and relative humidity were provided by the Nanyue Meteorological Station.

3 Results and discussion

3.1 Size-resolved ionic composition

The concentrations of PM_{10} from MOUDI (sum of the particulate matters that are equal to and less than 10 μm in aerodynamic diameter) at Mount Heng in spring are shown as a time series in Fig. 2. Generally, the PM_{10} concentration was relatively low at high elevations in South Central China. However, when the NG air masses dominated, heavy dust storms occurred, and the PM_{10} concentration increased by several times with coarse particles dominating the particulate matter. The average PM_{10} concentration was 152.0 μg$\cdot m^{-3}$, with the lowest value of 29.6 μg$\cdot m^{-3}$ under the NWC air masses and highest value of 749.3 μg $\cdot m^{-3}$ appearing during the dust-storm event. The aerosol concentrations and size distributions during the dust storm were greatly different from those during the periods without a dust storm; therefore, in most cases in this paper, the data were analyzed individually for the non-dust-storm periods (NDS) and dust-storm events (DS). The dust-storm periods were identified based on the following criteria: 1) the air masses were mainly from the north Gobi areas; 2) the PM_{10} concentration was above 100 μg$\cdot m^{-3}$ and 3) more than two thirds of PM_{10} existed in the coarse mode.

Because there is no 2.5 μm cut-point diameter in the MOUDI, the diameter of 1.8 μm was selected as the cut point to divide the fine and coarse particles. The average aerosol and ion mass concentrations in $PM_{1.8}$ and $PM_{1.8–10}$ and the $PM_{1.8}/PM_{10}$ ratios for the NDS and DS periods in the spring of 2009 at Mount Heng are listed in Table 1. On the NDS days, the mean $PM_{1.8}$ and $PM_{1.8–10}$ concentrations were 41.8 and 34.0 μg$\cdot m^{-3}$, respectively, with a $PM_{1.8}/PM_{10}$ ratio of 0.55. The mean fine sulfate, nitrate, and ammonium ion concentrations were 12.55, 1.66 and 5.34 μg$\cdot m^{-3}$, respectively. The sum of these three secondary inorganic ions accounted for 91.2% of the total water-soluble ions and contributed to 46.8% of the $PM_{1.8}$, indicating the dominant role of secondary inorganic ions in the fine particles. The mean fine potassium, sodium, and chloride ion concentrations were 0.63, 0.21, and 0.16 μg $\cdot m^{-3}$, respectively. The content of crustal substances (Ca^{2+}, Mg^{2+}, and F^-) in the fine particles was very small, ranging from 0.04 to 0.13 μg$\cdot m^{-3}$. The concentrations of most organic acids (i.e., formic acid, acetic acid, and MSA) in the fine particles were also very low, in the level of 0.05–0.12 μg$\cdot m^{-3}$, except for the oxalate acid, which was up to 0.44 μg$\cdot m^{-3}$. Overall, during the non-dust-storm periods at Mount Heng, sulfates, ammonium, potassium, MSA, and oxalate acid were primarily produced in the fine particles, with $PM_{1.8}/PM_{10}$ ratios of 82%–98%. Up to 93% of the potassium ions were produced in the fine mode, demonstrating that the aerosol potassium mainly came from anthropogenic sources (e.g., biomass burning) instead of soil dust [30]. More than half of the formic and acetic acids were produced in the fine mode, whereas only approximately one-third of the nitrates, chlorides, and sodium formed in the fine particles. The crustal ions mostly existed in the coarse mode. In contrast, in dust-storm events, the coarse particles dominated the particulate matter, and more aerosol ions were produced in the coarse mode. For example, the $PM_{1.8}/PM_{10}$ ratio of sulfates decreased from 94% to 63%, and that of nitrates from 34% to 11%. During the dust storm, the insoluble crustal substance dominated the aerosols. The secondary inorganic ions of sulfate, nitrate, and ammonium only amounted to 29.9% of the fine particles.

The size-resolved aerosol concentrations and chemical composition at Mount Heng to a certain degree reflected the characteristics of particulate matter pollution in the upper boundary layer in South Central China. These characteristics were likely different from that in the upper boundary layer in densely populated industrial region in North China. For comparison, the average aerosol and ion mass concentrations in $PM_{1.8}$ and $PM_{1.8–10}$ and the $PM_{1.8}/PM_{10}$ ratios for the NDS and NDS periods in spring 2007 at Mount Tai (1534 m asl, located in the North China Plain) are also listed in Table 1. Compared with Mount Tai, the concentrations of both $PM_{1.8}$ and $PM_{1.8–10}$ and almost all

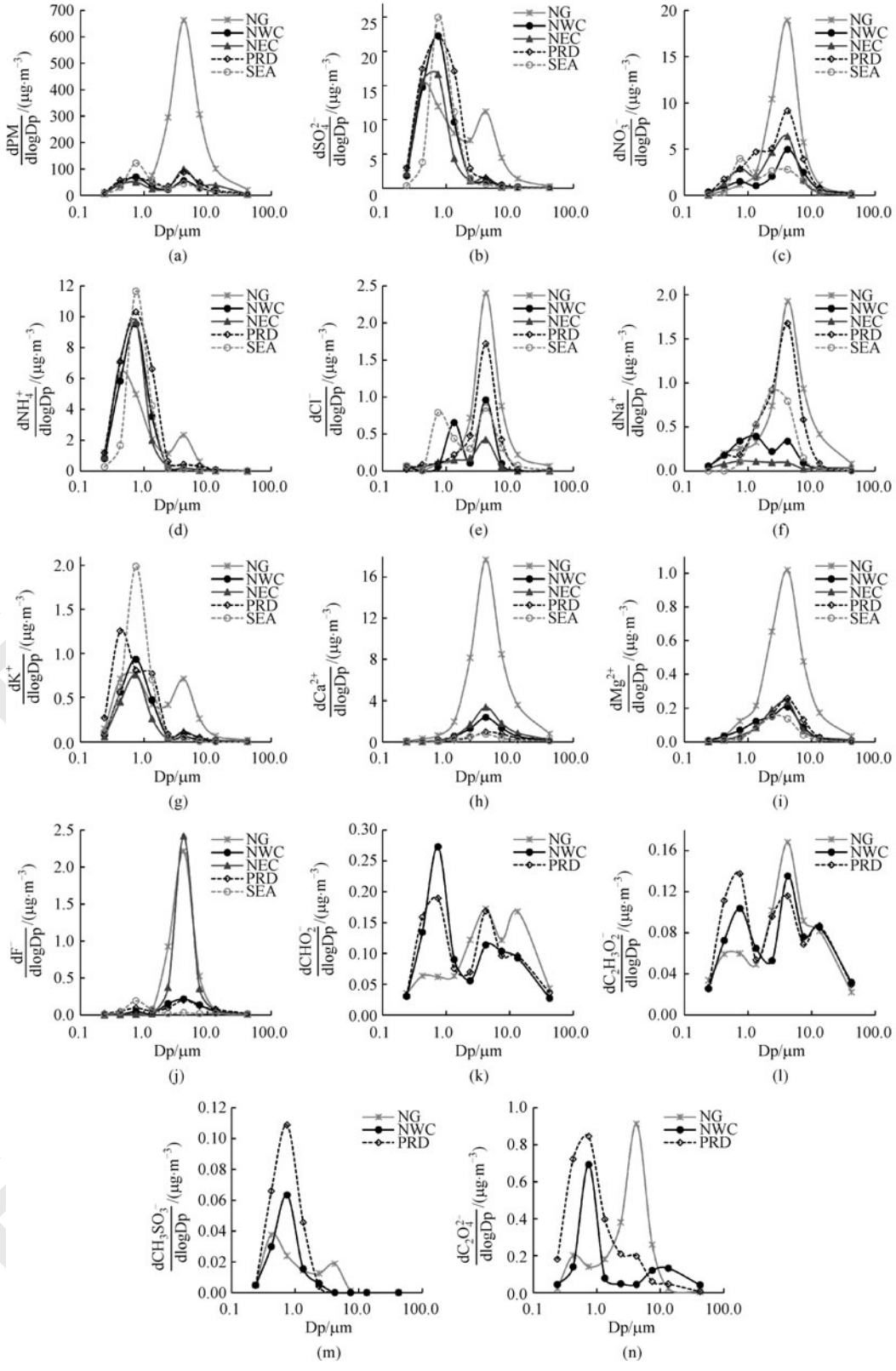

Fig. 3 Mean mass size distributions of aerosols and inorganic and organic water-soluble ions under five types of air masses in spring at Mount Heng: (a) PM; (b) SO_4^{2-}; (c) NO_3^-; (d) NH_4^+; (e) Cl^-; (f) Na^+; (g) K^+; (h) Ca^{2+}; (i) Mg^{2+}; (j) F^-; (k) CHO_2^-; (l) $C_2H_3O_2^-$; (m) $CH_3SO_3^-$; (n) $C_2O_4^{2-}$

water-soluble ions at Mount Heng were substantially lower. This result suggests that the particulate matter pollution in the upper boundary layer in South Central China was lighter than that in the North China Plain. Furthermore, for both the NDS and DS periods, the $PM_{1.8}/PM_{10}$ ratios of the secondary ions of sulfate and ammonium at Mount Heng were higher than those at Mount Tai, whereas the $PM_{1.8}/PM_{10}$ ratios of the primary ions of chloride, sodium, calcium, magnesium, and fluoride were lower than those at Mount Tai. The partition of aerosol components in the fine and coarse modes at Mount Heng was closer to the initial size distributions when they were immediately produced, indicating that the ambient aerosols at Mount Heng experienced fewer aging processes and were influenced by fewer anthropogenic emissions.

3.2 Size distributions of aerosol ions under different air masses

The high-elevation mountain site of Mount Heng features rare local anthropogenic emissions. Thus, the long-range transport of air masses likely has a significant influence on the concentrations and size distributions of aerosol ions at Mount Heng. During the periods dominated by the NG, NWC, NEC, PRD, and SEA air masses, the average mass size distributions of aerosols and inorganic and organic water-soluble ions are depicted in Fig. 3. The corresponding average trace gas concentrations and meteorological parameters are listed in Table 2. The data of NO_2 and O_3 were unavailable for the SEA air masses, because these two analyzers were not ready in the beginning of the field campaign when SEA air masses prevailed. On the sampling days except the dust-storm events (i.e., the NG air mass-dominated periods), the sulfate, ammonium, potassium, MSA, and oxalic ions exhibited a single concentration peak at 0.56–1.0 μm in the droplet mode. The sulfates were dominated by the droplet mode, which suggests that the dominant formation pathway of heterogeneous aqueous reactions occurs on aerosol surfaces and/or cloud processes under humid conditions [9,31,32]. This

Table 1 Mean aerosol and ion mass concentrations in $PM_{1.8}$ and $PM_{1.8–10}$ and the $PM_{1.8}/PM_{10}$ ratios for the NDS and DS days in spring 2009 at Mount Heng and in spring 2007 at Mount Tai ($\mu g \cdot m^{-3}$)

	Mount Heng (2009)						Mount Tai (2007)					
	NDS (n = 19)			DS (n = 7)			NDS (n = 10)			DS (n = 1)		
	$PM_{1.8}$	$PM_{1.8–10}$	$PM_{1.8}/PM_{10}$	$PM_{1.8}$	$PM_{1.8–10}$	$PM_{1.8}/PM_{10}$	$PM_{1.8}$	$PM_{1.8–10}$	$PM_{1.8}/PM_{10}$	$PM_{1.8}$	$PM_{1.8–10}$	$PM_{1.8}/PM_{10}$
PM	41.8	34.0	0.55	47.2	311.9	0.13	65.4	53.1	0.55	90.6	475.9	0.16
SO_4^{2-}	12.55	0.84	0.94	9.45	5.59	0.63	15.31	3.76	0.80	8.60	16.98	0.34
NO_3^-	1.66	3.17	0.34	1.07	8.64	0.11	8.12	4.37	0.65	2.05	7.04	0.23
NH_4^+	5.34	0.20	0.96	3.60	1.00	0.78	7.87	0.88	0.90	1.49	0.76	0.66
K^+	0.63	0.05	0.93	0.51	0.34	0.60	1.24	0.23	0.84	1.18	0.62	0.66
Na^+	0.21	0.40	0.34	0.21	0.89	0.19	0.32	0.25	0.56	0.70	4.59	0.13
Cl^-	0.16	0.40	0.29	0.09	0.98	0.08	0.90	0.40	0.69	0.54	1.74	0.24
Ca^{2+}	0.13	0.96	0.12	0.76	8.47	0.08	0.54	2.87	0.16	3.22	16.57	0.16
Mg^{2+}	0.04	0.12	0.26	0.10	0.53	0.15	0.15	0.27	0.37	0.38	1.02	0.27
F^-	0.04	0.17	0.19	0.02	0.90	0.03	0.04	0.14	0.22	0.05	0.20	0.19
CHO_2^-	0.12	0.08	0.61	0.06	0.10	0.35						
$C_2H_3O_2^-$	0.08	0.07	0.53	0.05	0.09	0.36						
$CH_3SO_3^-$	0.05	0.00	0.98	0.02	0.01	0.72						
$C_2O_4^{2-}$	0.44	0.09	0.82	0.14	0.38	0.26						

Table 2 Mean concentrations of SO_2, NO_2 and O_3 together with the mean ambient temperature and relative humidity for five types of air masses

air mass	SO_2 /ppbv	NO_2 /ppbv	O_3 /ppbv	temperature /°C	RH /%
NG	4.40	1.28	67.73	13.71	70.89
NWC	3.05	0.74	65.47	15.36	71.55
NEC	3.13	1.13	72.15	16.81	72.00
PRD	3.24	1.00	66.45	19.09	84.11
SEA	0.50			16.67	90.67

observation is different from the fine sulfates in spring at Mount Tai [21], which were dominated by the condensation mode and mainly produced via homogeneous oxidation followed by nucleation or condensation growth on existing aerosols. Calcium and magnesium showed a sole concentration peak at 3.2–5.6 μm in the coarse mode, whereas nitrates, chlorides, sodium, and fluorides generally had a major concentration peak in the coarse mode and a minor peak in the fine mode. Different from other water soluble ions, the size distributions of formic and acetic ions featured a second minor coarse concentration peak in the size range from 10 to 18 μm, suggesting there could be efficient formation of formates and acetates in this size bin.

Southeast Asia, the source region of the SEA air masses, was characterized by a large amount of biomass burning in March [24]. When the SEA air masses dominated, the concentrations of fine aerosols, sulfates, nitrates, ammonium, potassium, chlorides, and fluorides were significantly higher than those on other sampling days. Therefore, biomass burning contributed to the high concentrations of secondary inorganic aerosols in spring at Mount Heng. In addition, on the days dominated by the PRD air masses, elevated levels of sodium, chloride, and nitrates were observed in the coarse mode, indicating abundant sea salts in the coarse particles and fast coarse nitrate formation on the marine aerosols. The concurrently increased MSA concentration was due to abundant dimethyl sulfide and its subsequent oxidation by radicals in the marine air masses.

When the NG air masses prevailed, the air masses brought a large amount of dust from the Gobi desert to South China, and light and heavy dust storms were observed at Mount Heng. As shown in Fig. 3, during the dust storm, the mass size distributions of aerosols, nitrate, chloride, fluoride, sodium, calcium, and magnesium exhibited a single high concentration peak in the coarse mode. Moreover, the secondary ions of sulfate, ammonium, MSA and oxalate, which were primarily produced in the fine particles during non-dust-storm periods, also showed an apparent concentration peak in the coarse particles. These results indicate that the vast aerosol surface area of dusts was favorable to the secondary formation of coarse sulfates, ammonium, MSA, and oxalates via heterogeneous reactions on the dust surface. In particular, during the non-dust-storm periods the oxalates were primarily produced in the fine mode, whereas in the dust-storm events, they mostly formed in the coarse mode. In addition, during the dust storm the fine concentration peaks of sulfate, ammonium, MSA, and oxalate shifted to a smaller size – the condensation mode (0.32–0.56 μm). When the dust storm occurred, the RH was relatively low, and the fine aerosols were dominated by crustal substances. As a result, there was rare liquid water on the surfaces of the fine particles. The fine sulfates, ammonium, MSA, and oxalates were mainly produced via heterogeneous surface reactions on dry aerosols instead of wet aerosols or liquid droplets and thus existed in the smaller particles.

3.3 Secondary formation of sulfates and nitrates in fine and coarse modes

The secondary components of sulfate, nitrate, and ammonium were the major inorganic ions in the fine particles and also appeared in the coarse particles, particularly during the dust storm. They were mostly produced from anthropogenic precursors via a series of physical and chemical processes. To gain an understanding of the formation mechanisms and influencing factors, the sulfates and nitrates in different size ranges were analyzed in detail in conjugation with the related air pollutants and weather parameters.

3.3.1 Fine-mode sulfates and nitrates

Figure 4(a) shows the linear regression curve between ammonium and sulfate in size bins in the fine mode (i.e., 0.18–0.32 μm, 0.32–0.56 μm, 0.56–1.0 μm, and 1.0–1.8 μm) in spring at Mount Heng. The strong correlation (R^2 = 0.89) demonstrates that the fine sulfates always coexisted with ammonium. Generally, the molar concentrations of fine ammonium were 2.24 ($p < 0.0001$ for the t-test of the slope) times that of sulfate, indicating that the fine sulfates were fully neutralized by the ammonium ions and primarily existed in the form of $(NH_4)_2SO_4$. The remaining small part of the ammonium ions possibly coexisted with the anions of nitrate and chloride. During the non-dust-storm periods at Mount Heng, the fine sulfates were primarily produced via heterogeneous aqueous oxidation of SO_2 on the surfaces of wet aerosols or liquid droplets. The production rate and concentration of fine sulfate were mainly controlled by the concentrations of gaseous precursors (SO_2 and oxidants), aerosol surface area, and the liquid water content on the aerosol/droplet surfaces. Because there were few SO_2 emission sources locally, the ambient SO_2 concentration was relatively low (average 3.0 ppbv for the NDS periods) and not variable. The ambient air was humid (average 78.6%), and thus there was always liquid water on the surface of fine aerosols. As a result, the aerosol surface area was likely the dominant factor that influenced the fine sulfate concentration, which is indicated by the good positive correlation between fine sulfate and fine aerosol loading (R^2 = 0.79, shown in Fig. 4(b)). This result is different from the humidity-dependent heterogeneous formation of fine sulfates in urban areas in the North China Plain [33]. During the dust storm, the average SO_2 concentration was 4.4 ppbv, approximately 1.5 times the value of 3.0 ppbv during the non-dust-storm periods. However, the linear slope between the fine sulfate and fine PM for the DS was much lower than that for the NDS (see Fig. 4(b)), suggesting a slower production rate of fine sulfate on dry aerosol surfaces during dust-storm events.

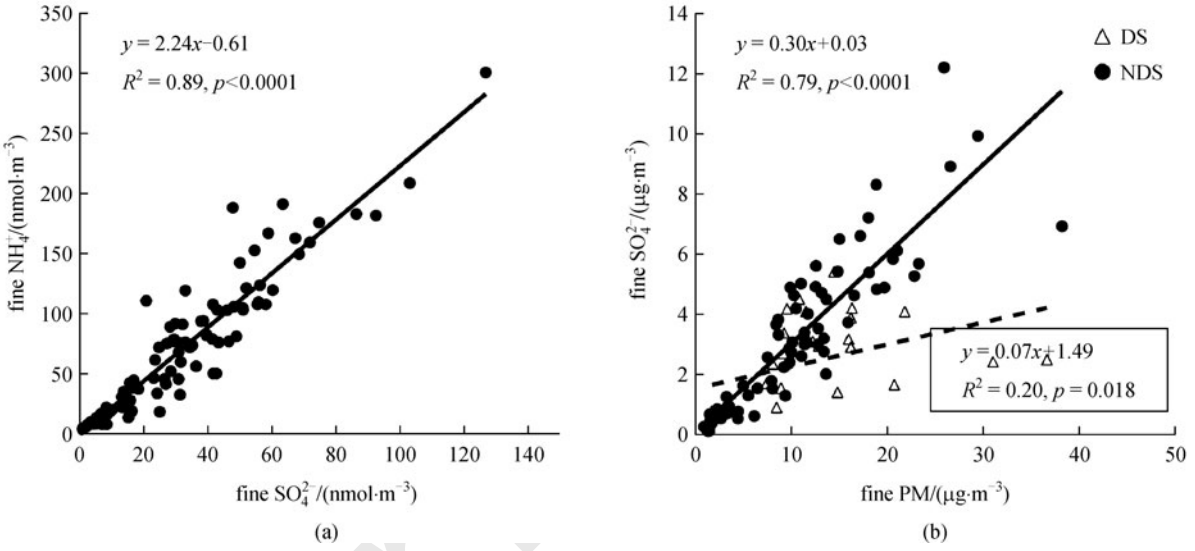

Fig. 4 Linear regression curves of (a) ammonium vs. sulfate (molar concentration) and (b) sulfate vs. particulate matter (mass concentration) in size bins in the fine mode

The concentrations of fine nitrate were substantially low in spring at Mount Heng. The nitrates were mostly produced in coarse particles, indicating that Mount Heng was an ammonia-poor environment in spring and that there was scarcely excess ammonia to react with nitric acid to produce ammonium nitrates in fine particles. This observation differs from that at Mount Tai – the nitrates mostly formed in fine particles in the form of NH_4NO_3 [21]. Different from fine sulfates, the fine nitrates had only a weak correlation with the fine aerosol loading, but a moderate correlation (R^2 = 0.34) with the ambient relative humidity (data not shown here). The fine nitrate concentration tended to increase with rising RH. When the RH was 50%–70%, 70%–80%, 80%–90%, and 90%–100%, the fine nitrate concentration was 0.58, 1.57, 1.71, and 3.05 $\mu g \cdot m^{-3}$, respectively. These results demonstrate that the ambient humidity was most likely the dominant factor that influenced the secondary formation of fine nitrate via the heterogeneous uptake of gaseous nitric acid and/or dinitrogen pentoxide [34,35].

3.3.2 Coarse-mode sulfates and nitrates

During non-dust-storm periods at Mount Heng, the concentrations of coarse sulfate and ammonium were generally low, averaging 0.84 and 0.20 $\mu g \cdot m^{-3}$, respectively. In the dust-storm events, the coarse sulfate and ammonium concentrations increased to 5.59 and 1.00 $\mu g \cdot m^{-3}$, respectively, which were more than five times the values during non-dust-storm periods (see Table 1). During the dust storm, the sulfates and ammonium exhibited a remarkable concentration peak in the coarse mode and the coarse peak of ammonium only appeared when the sulfates had a coarse peak, suggesting that the coarse-mode ammonium primarily coexisted with the sulfates. Figures 5(a) and 5(b) show the linear regression curves of sulfates and ammonium with the particulate matter in size bins in the coarse mode (i.e., 1.8–3.2 μm, 3.2–5.6 μm, 5.6–10 μm, 10–18 μm, and 18–100 μm) for the DS and NDS periods. The elevated levels of coarse sulfates and ammonium appearing in dust-storm events were well-correlated with the dust loading (R^2 = 0.88 and 0.74, respectively), which indicates that the coarse sulfates and ammonium mainly formed via heterogeneous reactions/uptake of SO_2 and NH_3 on the dust surface and largely depended on the surface area. The linear slope between the coarse sulfates and aerosol loading for the DS was similar to that for the NDS. However, the slope between coarse ammonium and aerosol loading for the DS was significantly smaller than that for the NDS (0.003 vs. 0.005). The lower molar ratios of NH_4^+/SO_4^{2-} (< 1.0) during dust-storm events (see Fig. 5(c)) further demonstrated that the heterogeneous uptake of NH_3 on alkaline dusts was less efficient than that on the coarse particles during the non-dust-storm periods.

Approximately two-thirds of the nitrates were in the coarse particles. As shown in Fig. 6, there were strong positive correlations between the coarse nitrates and coarse particle concentrations for both the DS and NDS periods (R = 0.89 and 0.56, respectively), suggesting that the secondary formation of coarse nitrates was governed by the coarse particle loading (i.e., the aerosol surface area). Although the average NO_2 concentration (1.28 ppbv) during dust-storm events was 1.3 times the value during non-dust-storm periods, the linear slope between the coarse nitrate and the coarse PM for the DS was approximately one fifth of that for the NDS, indicating that the production rate of coarse nitrate on dry dusts was relatively slow.

As described previously, the elevated concentrations of

coarse nitrate appeared when the sea salt was abundant. During the non-dust-storm periods at Mount Heng, coarse nitrate was well-correlated (R^2 = 0.68) with the content of coarse sodium, and the chloride concentration was approximately one-half of the sodium concentration in the coarse mode (as shown in Fig. 7). These results suggest that the heterogeneous uptake of nitric acid and/or dinitrogen pentoxide on sea salts facilitated the secondary formation of coarse nitrate and led to a significant depletion of chlorides.

4 Summary and conclusions

Size-segregated aerosol samples were collected using MOUDI at Mount Heng in South Central China in spring 2009, followed by subsequent gravimetric and ionic analyses in the laboratory. During the sampling period, the mean fine and coarse particle concentrations on the non-dust-storm days were 41.8 and 34.0 μg·m^{-3}, respectively, with a $PM_{1.8}/PM_{10}$ ratio of 0.55. Compared with Mount Tai in the North China Plain, the average mass concentrations of aerosols and water-soluble ions in both the fine and coarse modes at Mount Heng were apparently lower, indicating that the upper boundary layer in South Central China experienced lighter particulate matter pollution than that in the North China Plain. In spring at Mount Heng, the sulfates, ammonium, potassium, MSA, and oxalates were primarily produced in fine particles with a concentration peak appearing in the droplet mode (0.56–1.0 μm), whereas calcium and magnesium were mostly distributed in the coarse particles with a concentration peak occurring in the size range of 3.2–5.6 μm. The nitrates, chlorides, sodium, fluorides, formates, and acetates showed obvious concentration peaks in both the fine and coarse modes. Influenced by biomass burning in the Southeast Asia region, elevated concentrations of fine sulfates, nitrates, ammonium, potassium, chloride, and fluorides

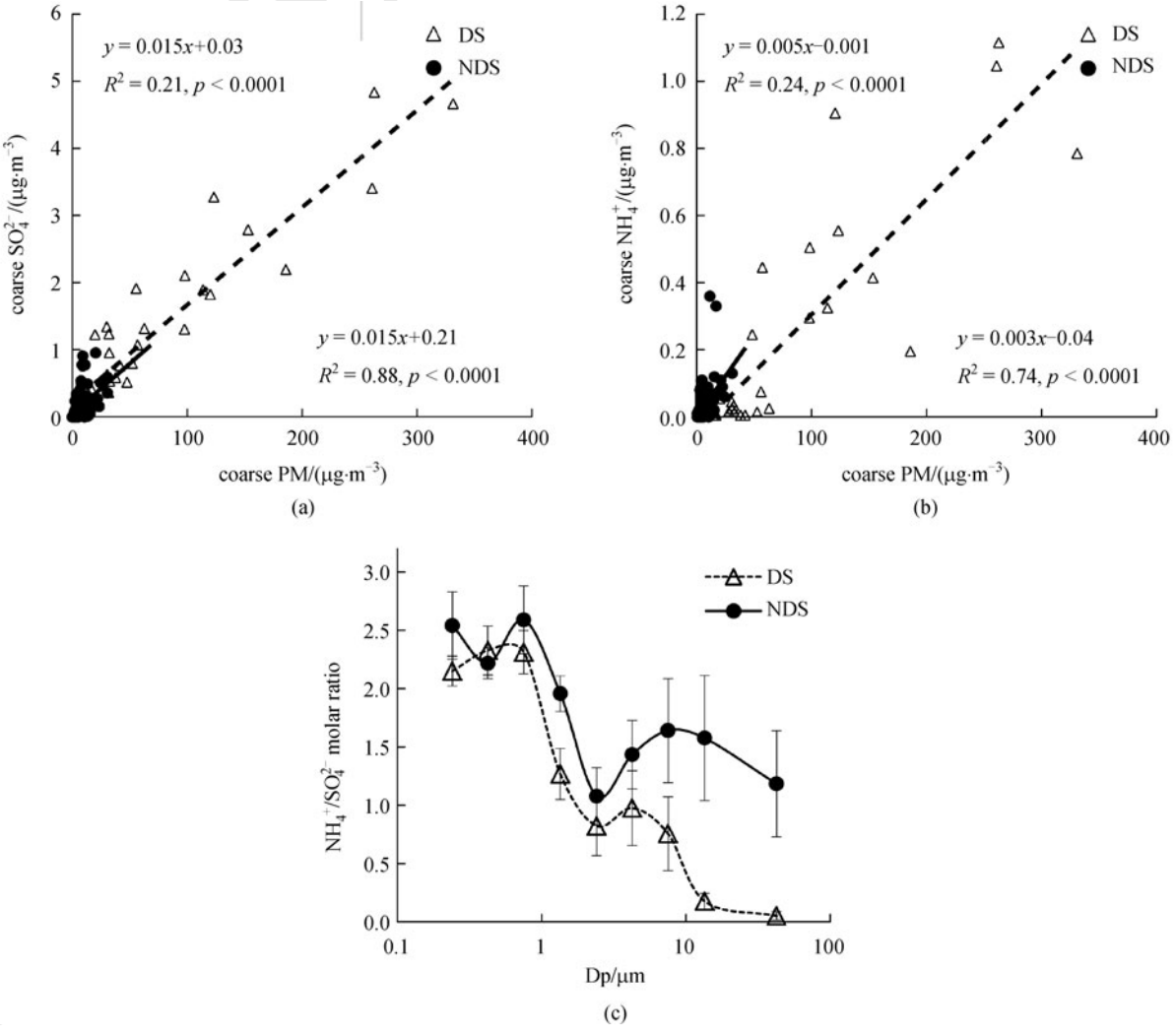

Fig. 5 Linear regression curves of (a) sulfate vs. particulate matter and (b) ammonium vs. particulate matter in size bins in the coarse mode and (c) the molar ratios of ammonium to sulfate in different size bins for the DS and NDS periods

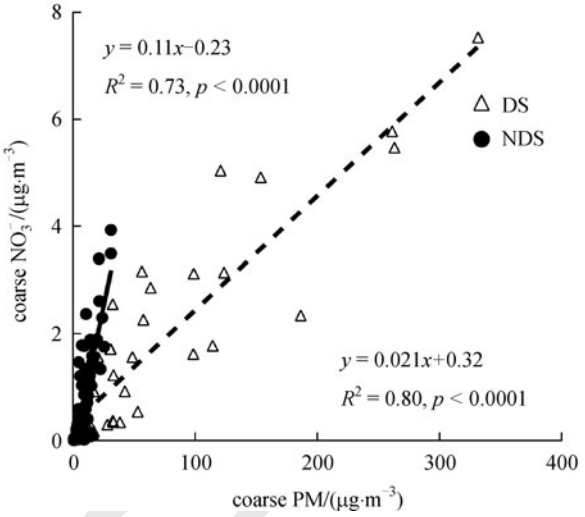

Fig. 6 Linear regression curves of nitrate vs. particulate matter in size bins in the coarse mode for the DS and NDS periods

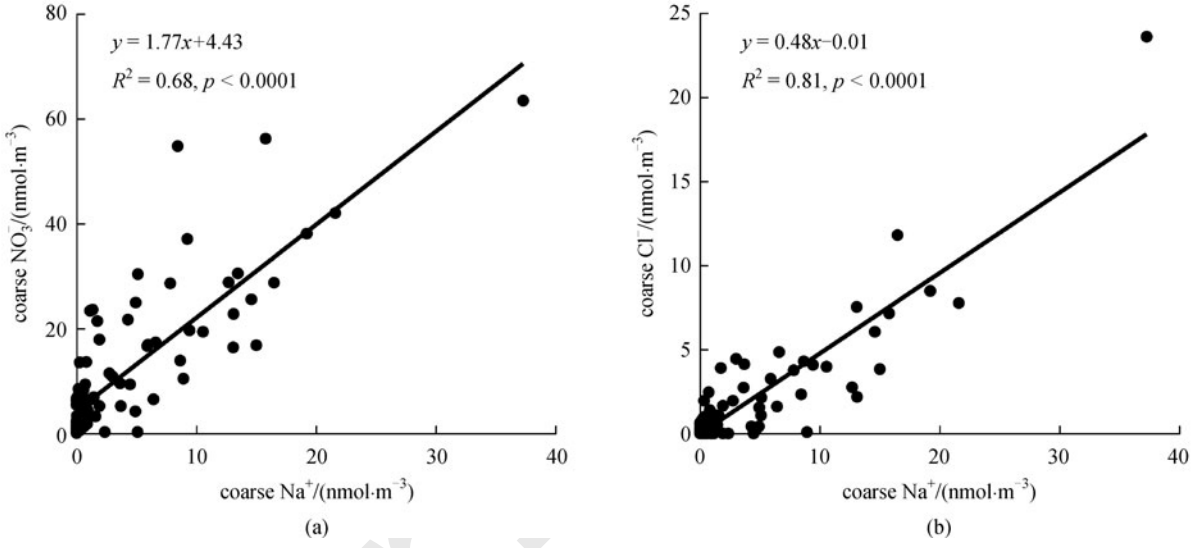

Fig. 7 Linear regression curves of (a) nitrate vs. sodium and (b) chloride vs. sodium in size bins in the coarse mode during the non-dust-storm periods

were observed when the SEA air masses prevailed. The fine sulfates were mostly distributed in the droplet mode and existed in the form of $(NH_4)_2SO_4$. They were mainly produced via heterogeneous aqueous reactions and/or cloud processes, and the concentration was governed by fine aerosol loading. The nitrates mostly formed in the coarse mode. The fine nitrate concentration was increased with rising RH, whereas the coarse nitrates correlated well with the coarse aerosol loading. In addition, when the air masses form the north Gobi prevailed, light and heavy dust storms were observed at Mount Heng, characterized by extremely high levels of coarse particles and elevated concentrations of secondary ions of sulfate, nitrate, ammonium, and oxalate in the coarse mode. During the dust storm, the vast aerosol surface area led to a significant production of coarse sulfates, nitrates, and ammonium; however, the formation of coarse nitrates and ammonium via the heterogeneous uptake of nitric acid and ammonia on dry alkaline dusts was less efficient than that on the coarse particles the during non-dust-storm periods.

Acknowledgements This work was supported by the National Key Basic Research Program of China (Grant No. 2005CB422203), the Niche Area Development Program of the Hong Kong Polytechnic University (1-BB94), the Shandong Provincial Environmental Protection Bureau (2006045) and the Special Research for Public-Beneficial Environment Protection (201009001-1). The authors thank Chao Yuan, Zheng Xu, Shengzhen Zhou, and Rui Gao for their contributions to the sample analysis and field work.

References

1. Yang F, Tan J, Zhao Q, Du Z, He K, Ma Y, Duan F, Chen G, Zhao Q. Characteristics of $PM_{2.5}$ speciation in representative megacities and across China. Atmospheric Chemistry and Physics, 2011, 11 (11): 5207–5219
2. Pitchford M, Maim W, Schichtel B, Kumar N, Lowenthal D, Hand J. Revised algorithm for estimating light extinction from IMPROVE particle speciation data. Journal of the Air & Waste Management Association, 2007, 57(11): 1326–1336
3. Topping D O, McFiggans G. Tight coupling of particle size, number and composition in atmospheric cloud droplet activation. Atmospheric Chemistry and Physics, 2012, 12(7): 3253–3260
4. Tang A, Zhuang G, Wang Y, Yuan H, Sun Y. The chemistry of precipitation and its relation to aerosol in Beijing. Atmospheric Environment, 2005, 39(19): 3397–3406
5. Salma I, Balashazy I, Winkler-Heil R, Hofmann W, Zaray G. Effect of particle mass size distribution on the deposition of aerosols in the human respiratory system. Journal of Aerosol Science, 2002, 33(1): 119–132
6. Cheng S, Yang L, Zhou X, Wang Z, Zhou Y, Gao X, Nie W, Wang X, Xu P, Wang W. Evaluating $PM_{2.5}$ ionic components and source apportionment in Jinan, China from 2004 to 2008 using trajectory statistical methods. Journal of Environmental Monitoring, 2011, 13 (6): 1662–1671
7. Zhang M, Chen J M, Wang T, Cheng T T, Lin L, Bhatia R S, Hanvey M. Chemical characterization of aerosols over the Atlantic Ocean and the Pacific Ocean during two cruises in 2007 and 2008. Journal of Geophysical Research, 2010, 115(D22): D22302, doi: 10.1029/2010JD014246
8. Mori I, Nishikawa M, Tanimura T, Quan H. Change in size distribution and chemical composition of kosa (Asian dust) aerosol during long-range transport. Atmospheric Environment, 2003, 37 (30): 4253–4263
9. Seinfeld J H, Pandis S N. Atmospheric Chemistry and Physics: from Air Pollution to Climate Change. 2nd ed. New York: John Willey & Sons, Inc., 2006
10. Liu S, Hu M, Slanina S, He L Y, Niu Y W, Bruegemann E, Gnauk T, Herrmann H. Size distribution and source analysis of ionic compositions of aerosols in polluted periods at Xinken in Pearl River Delta (PRD) of China. Atmospheric Environment, 2008, 42 (25): 6284–6295
11. Horemans B, Krata A, Buczynska A J, Dirtu A C, van Meel K, van Grieken R, Bencs L. Major ionic species in size-segregated aerosols and associated gaseous pollutants at a coastal site on the Belgian North Sea. Journal of Environmental Monitoring, 2009, 11(3): 670–677
12. Guo S, Hu M, Wang Z B, Slanina J, Zhao Y L. Size-resolved aerosol water-soluble ionic compositions in the summer of Beijing: implication of regional secondary formation. Atmospheric Chemistry and Physics, 2010, 10(3): 947–959
13. Li J, Wang G, Zhou B, Cheng C, Cao J, Shen Z, An Z. Chemical composition and size distribution of wintertime aerosols in the atmosphere of Mt. Hua in central China. Atmospheric Environment, 2011, 45(6): 1251–1258
14. Cheng S, Yang L, Zhou X, Xue L, Gao X, Zhou Y, Wang W. Size-fractionated water-soluble ions, situ pH and water content in aerosol on hazy days and the influences on visibility impairment in Jinan, China. Atmospheric Environment, 2011, 45(27): 4631–4640
15. Wang G, Li J, Cheng C, Hu S, Xie M, Gao S, Zhou B, Dai W, Cao J, An Z. Observation of atmospheric aerosols at Mt. Hua and Mt. Tai in central and east China during spring 2009 – Part 1: EC, OC and inorganic ions. Atmospheric Chemistry and Physics, 2011, 11(9): 4221–4235
16. Zhang Q, Jimenez J L, Canagaratna M R, Allan J D, Coe H, Ulbrich I, Alfarra M R, Takami A, Middlebrook A M, Sun Y L, Dzepina K, Dunlea E, Docherty K, DeCarlo P F, Salcedo D, Onasch T, Jayne J T, Miyoshi T, Shimono A, Hatakeyama S, Takegawa N, Kondo Y, Schneider J, Drewnick F, Borrmann S, Weimer S, Demerjian K, Williams P, Bower K, Bahreini R, Cottrell L, Griffin R J, Rautiainen J, Sun J Y, Zhang Y M, Worsnop D R. Ubiquity and dominance of oxygenated species in organic aerosols in anthropogenically-influenced Northern Hemisphere midlatitudes. Geophysical Research Letters, 2007, 34(13): L13801, doi: 10.1029/2010JD014246
17. Yao X H, Lau A P S, Fang M, Chan C K, Hu M. Size distributions and formation of ionic species in atmospheric particulate pollutants in Beijing, China: 1–inorganic ions. Atmospheric Environment, 2003, 37(21): 2991–3000
18. Hu M, Zhao Y L, He L Y, Huang X F, Tang X Y, Yao X H, Chan C K. Mass size distribution of Beijing particulate matters and its inorganic water-soluble ions in winter and summer. Environmental Sciences, 2005, 26(4): 1–6 (in Chinease)
19. Zhao P, Zhu T, Liang B, Hu M, Kang L, Gong J. Characteristics of mass distributions of aerosol particle and its inorganic water-soluble ions in summer over a suburb farmland in Beijing. Frontiers of Environmental Science & Engineering in China, 2007, 1(2): 159–165
20. Huang X F, Yu J, He L Y, Yuan Z. Water-soluble organic carbon and oxalate in aerosols at a coastal urban site in China: size distribution characteristics, sources and formation mechanisms. Journal of Geophysical Research, 2006, 111(D22): D22212, doi: 10.1029/2006JD007408
21. Gao X, Wang T, Zhou Y, Xue L, Zhang Q, Wang X, Nie W, Wang W, Wang D. Size distribution of atmospheric particles and water soluble inorganic ions in spring and summer at Mount Tai. Environmental Chemistry, 2011, 30(3): 686–692 (in Chinese)
22. Ding Y. Monsoons over China. Norwell: Kluwer Acad., 1994
23. Fuelberg H E, Kiley C M, Hannan J R, Westberg D J, Avery M A, Newell R E. Meteorological conditions and transport pathways during the Transport and Chemical Evolution over the Pacific (TRACE-P) experiment. Journal of Geophysical Research, 2003, 108(D20): 8782, doi: 10.1029/2002JD003092
24. Zhou S, Wang Z, Gao R, Xue L, Yuan C, Wang T, Gao X, Wang X, Nie W, Xu Z, Zhang Q, Wang W. Formation of secondary organic carbon and long-range transport of carbonaceous aerosols at Mount Heng in South China. Atmospheric Environment, 2012, 63(2012): 203–212
25. Zhang Q, Streets D G, Carmichael G R, He K, Huo H, Kannari A, Klimont Z, Park I, Reddy S, Fu J, Chen D, Duan L, Lei Y, Wang L T, Yao Z L. Asian emissions in 2006 for the NASA INTEX-B mission. Atmospheric Chemistry and Physics, 2009, 9(14): 5131–5153

26. Zhang M, Wang S, Wu F, Yuan X, Zhang Y. Chemical compositions of wet precipitation and anthropogenic influences at a developing urban site in southeastern China. Atmospheric Research, 2007, 84 (4): 311–322
27. Sun M, Wang Y, Wang T, Fan S, Wang W, Li P, Guo J, Li Y. Cloud and the corresponding precipitation chemistry in south China: water-soluble components and pollution transport. Journal of Geophysical Research, 2010, 115(D22): D22303, doi: 10.1029/2010JD014315
28. Draxler R R, Rolph G D. HYSPLIT (HYbrid Single-Particle Lagrangian Integrated Trajectory). Silver Spring, MD: NOAA Air Resources Laboratory, 2012. Available online at http://ready.arl.noaa.gov/HYSPLIT.php (accessed September 26, 2012)
29. Gao X, Xue L, Wang X, Wang T, Yuan C, Gao R, Zhou Y, Nie W, Zhang Q, Wang W. Aerosol ionic components at Mt. Heng in central southern China: abundances, size distribution, and impacts of long-range transport. Science of the Total Environment, 2012, 433(433): 498–506
30. Liu X, Van Espen P, Adams F, Cafmeyer J, Maenhaut W. Biomass burning in Southern Africa: individual particle characterization of atmospheric aerosols and savanna fire samples. Journal of Atmospheric Chemistry, 2000, 36(2): 135–155
31. Mather T, Allen A, Oppenheimer C, Pyle D, McGonigle A. Size-resolved characterisation of soluble ions in the particles in the tropospheric plume of Masaya volcano, Nicaragua: Origins and plume processing. Journal of Atmospheric Chemistry, 2003, 46(3): 207–237
32. Yao X H, Zhang L. Sulfate formation in atmospheric ultrafine particles at Canadian inland and coastal rural environments. Journal of Geophysical Research, 2011, 116(D10): D10202, doi: 10.1029/2010JD015315
33. Wang X, Wang W, Yang L, Gao X, Nie W, Yu Y, Xu P, Zhou Y, Wang Z. The secondary formation of inorganic aerosols in the droplet mode through heterogeneous aqueous reactions under haze conditions. Atmospheric Environment, 2012, 63(2012): 68–76
34. Wang X, Zhang Y, Chen H, Yang X, Chen J, Geng F. Particulate nitrate formation in a highly polluted urban area: a case study by single-particle mass spectrometry in Shanghai. Environmental Science & Technology, 2009, 43(9): 3061–3066
35. Ying Q. Physical and chemical processes of wintertime secondary nitrate aerosol formation. Frontiers of Environmental Science & Engineering in China, 2011, 5(3): 348–361